An Optimization of the Two-Echelon Vehicle Routing Problem with Drones Considering Truck Travel Time and Carbon Emissions

Santoso Santoso
Department of Industrial Systems and Engineering, Institut Teknologi Sepuluh Nopember, Surabaya, Indonesia | Industrial Engineering Department, Universitas Kristen Maranatha, Bandung, Indonesia
santoso@eng.maranatha.edu

Nurhadi Siswanto
Department of Industrial Systems and Engineering, Institut Teknologi Sepuluh Nopember, Surabaya, Indonesia
siswanto@ie.its.ac.id (corresponding author)

Budi Santosa
Department of Industrial Systems and Engineering, Institut Teknologi Sepuluh Nopember, Surabaya, Indonesia
budi_s@ie.its.ac.id

Budisantoso Wirjodirdjo
Department of Industrial Systems and Engineering, Institut Teknologi Sepuluh Nopember, Surabaya, Indonesia
santoso@ie.its.ac.id

Received: 6 April 2026 | Revised: 4 May 2026, 22 May 2026, and 24 May 2026 | Accepted: 1 June 2026

 DOI: https://doi.org/10.48084/etasr.19139

ABSTRACT

The Two-Echelon Vehicle Routing Problem with Drones (2E VRP-D) model can initiate flights from the truck, complete several deliveries to different customer locations, and then rendezvous with the truck again. In addition to economic benefits, logistics providers must consider the environmental impacts of the order-fulfillment process. A novel multi-objective optimization framework is established in this study to simultaneously minimize the total time required for truck travel while also reducing total carbon emissions. Due to restrictions in payload capacity and battery energy limits, drones need to work alongside trucks to deliver services effectively. A dynamic energy consumption model is applied for the drone, where energy use changes based on the loading rate, enabling a more realistic representation of actual operations. This complex problem is addressed using the Non-Dominated Sorting Genetic Algorithm (NSGA-II) with two approaches: the Giant Chromosome (GC) and K-means methods. Routing plans for both trucks and drones are then constructed using a novel heuristic algorithm. Overall, the K-means method delivers better average objective values, reflecting enhanced exploitation performance. Conversely, the GC method produces a higher Hypervolume (HV), indicating superior convergence and coverage of the Pareto front, supported by a lower spacing value, while K-means achieves a slightly better spread. These outcomes contribute to improving logistics operations and informing government policy decisions.

Keywords-carbon emission; logistics; multi-objective optimization; vehicle routing problem with drones

I. INTRODUCTION

The e-commerce sector and the increasing concentration in urban areas have led to a rise in demand for home delivery, placing significant pressure on last-mile logistics [1]. E-commerce and logistics businesses face substantial challenges in keeping pace with the exponential growth in customer demand. Unmanned Aerial Vehicles (UAVs), particularly drones, are among the most promising emerging technologies capable of satisfying customer demands for fast, flexible, and reliable delivery systems. Drones serve as a new delivery method that enables quick and convenient services. Unlike

traditional ground vehicles, drones do not rely on road systems or face traffic-related disruptions, which often cause delivery delays. Therefore, many leading technology companies and logistics service providers have explored and implemented drone-powered last-mile delivery services [2].

However, drones have a limited capacity, usually carrying only one or a small number of packages, and a restricted operating range, which necessitates repeated charging or battery replacement to maintain operations. Therefore, effective coordination between trucks and drones is essential to achieve cost-efficiency and high performance in delivery. Collaborative truck-drone delivery systems reduce costs, CO_2 emissions, and delivery time. A hybrid delivery system combining trucks and drones could be adopted by an industry in order to optimize its delivery operations, saving both time and energy [3]. However, the problem of truck-drone collaboration routing is structurally complex and has received limited attention in existing studies.

The innovation of lighter materials and more efficient batteries has expanded drone capabilities, allowing them to carry multiple packages simultaneously. In the Two-Echelon system (2E), drones are launched from a truck carrying several packages intended for various customers prior to regrouping with the truck [4]. This vehicle-drone routing framework, which relies on one truck, is the 2E Travelling Salesman Problem supported by Drones (2E TSP-D), whereas models involving multiple trucks are referred to as the 2E VRP-D. The focus of this research lies in the area of the 2E VRP-D.

In general, the methods used to solve 2E VRP-D problems include exact algorithms, heuristics, and machine learning techniques [5]. Several works rely on exact methods when dealing with small-scale instances [2, 6-12]. However, due to the complexity of larger problem instances, heuristic and metaheuristic approaches have been adopted. These include the Drone Truck Route Construction framework paired with the Large Neighborhood Search technique [2], SA combined with Tabu Search (TS) [13], Adaptive LNS [7], K-means-driven and Ant Colony Optimization-driven approaches [14], the Hybrid Evolutionary Algorithm and Ant Colony-based hybrid method [8], the Neighborhood Search heuristic [15], the Iterative Local Search-based algorithm [9], the Simulated Annealing approach [11], the Scanning and Heuristic Insertion Algorithm (SHIA) with the Enhanced Variable Neighborhood Search (EVNS) algorithm [12], the Multi-stage heuristic optimization algorithm [16], and the Hybrid Strategy-assisted Multi-objective Optimization Algorithm (HSMOA) [17]. The application of 2E VRP-D is widely carried out in the last-mile delivery sector [2, 6, 7, 9-13, 16, 17] and surveillance [15], as well as in the humanitarian sector [8, 14].

Transportation was the second biggest emitter of carbon globally in 2018, contributing 24.64%, according to the International Energy Agency, just behind the electricity and heat sector [18]. When used effectively, drone delivery can reduce both energy consumption and carbon emissions. Transportation is a crucial element of logistics operations, and providers are expected to evaluate both economic outcomes and ecological sustainability in the delivery process. Authors in [19] noted that a routing scheme with minimum total carbon emissions is not necessarily the one with the lowest economic cost. However, most current drone-related research focuses on a single objective. In real-world applications, multiple objectives should be considered simultaneously [20]. Real-world problems often involve multiple conflicting objectives, where optimizing a single objective may lead to suboptimal decisions. Multi-criteria optimization [21] enables the generation of a set of Pareto-optimal solutions, allowing decision-makers to evaluate trade-offs among objectives and select the most suitable solution. Among existing 2E VRP-D studies, only two have examined multiple objective functions, without addressing environmental impacts or delivery-related carbon emissions. Authors in [8] discussed a multi-objective approach that addresses goals such as minimizing the maximum cooperative routing time while maximizing the minimum fulfillment rate of request nodes, while authors in [17] focused on minimizing operational costs and workload imbalance of vehicle–drone formations. This study presents a bi-objective 2E-VRPD model that aims to minimize truck travel time and total carbon emissions, with the goal of identifying fast delivery routes that are also environmentally sustainable.

The assumption of a fixed flight range or time is common in drone operations. In reality, drones carrying lighter payloads have longer flight endurance compared to fully loaded ones. In [19] drone flight endurance was modeled as a linearly decreasing function of the loading rate, reaching 80% of the empty-drone endurance at full load level. Authors in [9] analyzed energy consumption in the 2E-VRPD model, measuring it based on varying flight time and payload. Their calculation included energy consumed during flight, customer service time, and when the drone was hovering or waiting. Authors in [10] investigated drone energy consumption within a 2E-VRPD framework, where energy depends on payload and is modeled nonlinearly. In this study, a 2E-VRP model was adopted, in which energy consumption was calculated based on both the carried payload and distance, as per the approach developed by [22]. The linear approximation of the drone energy consumption model is expected to provide computational efficiency for large-scale optimization.

Due to its computational complexity, in addition to exact methods, heuristic and metaheuristic approaches are often proposed [23]. The 2E-VRP model in this study employs the Non-Dominated Sorting Genetic Algorithm (NSGA-II) method. The adoption of NSGA-II to address multi-objective optimization challenges has been expanded, especially in the past five to six years [24]. The presence of complexity, nonlinearity, and non-convexity in the problem motivates the use of an elitist multi-objective optimization technique. As highlighted in [25], NSGA-II is particularly effective in handling such characteristics due to its fast non-dominated sorting mechanism and elitism strategy, which ensure convergence toward a well-distributed Pareto front. No existing research on the 2E VRP-D has employed the NSGA-II method to solve the problem. This study, therefore, applies NSGA-II to solve the proposed bi-objective 2E-VRPD.

II. MODEL DEVELOPMENT

The 2E VRP-D structure assumes a fleet of n trucks and n drones, ensuring that every truck operates with a single

dedicated drone. Drones are able to complete several deliveries independently before rejoining their assigned truck. The truck can simultaneously make its own deliveries and function as a moving intermediate depot. A drone can handle a number of packages and serve several demand locations per trip, within capacity and range limits. The objective is to serve all demand points precisely one time, through truck or drone-performed operations. The trucks are dispatched fully loaded from the depot and return empty. Each truck may perform only one round trip from and back to the depot. Drones cannot travel to or from the depot on their own. After completing a route and rejoining the truck, drones receive a fully recharged battery. Since the routing scheme that minimizes total carbon emissions is not necessarily the same as the one that minimizes economic cost, this study adopts a bi-objective approach: minimizing the truck's travel time and minimizing carbon emissions. The routing solution incorporating trucks and drones is depicted in Figure 1.

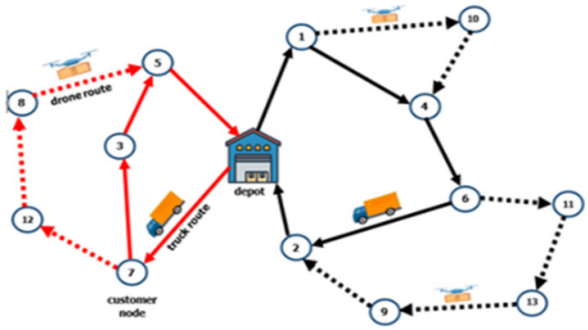

Fig. 1. An illustrative solution of the 2E-VRP-D, demonstrating the integration of truck routing and drone delivery operations.

Drones operate under battery life constraints that limit their flight time. The model employs the payload-weight-based energy consumption estimation developed by [22]. Both drones and trucks have their own capacity constraints. Drones are assumed to be incapable of taking off and landing at the same node simultaneously. Therefore, the truck–drone pair must synchronize at customer points, requiring mutual waiting if their arrival times differ. Each drone must go back to its originating truck and cannot be reassigned to another one. The travel distance of the truck and the drone will be measured using Manhattan and Euclidean distances, respectively.

The development of the 2E VRP-D model requires defining the sets, parameters, and variables listed below:

C: Set of customer locations to be served (i = 1, 2, 3, … n)

N: Set of all nodes including starting depot (0_s) and ending depot (0_r) = $\{0_s\} \cup C \{0_r\}$, where 0_s and 0_r refer to the same depot location.

C_0/C_+: Set of all customers plus the starting/ending depot, $C_0 = \{0_s\} \cup C$, $C_+ = \{0_r\} \cup C$.

v: Truck set (v = 0, 1, 2, 3, … v)

d: Drone set (d = 0, 1, 2, 3, … d)

Parameters required for the formulation:

T_{ij}: Time required between locations i and j using truck delivery (h).

T_{ij}^{d}: Time required between locations i and j using drone delivery (h).

d_{ij}: The Manhattan distance from location i to j (km).

G_i: The demand level for location i, where the demand at location 0 (depot) is 0 (kg).

Q^v: Maximum allowable load for truck v (kg).

Q^d: Maximum allowable load for drone d (kg).

M: A sufficiently large number.

E: Drone battery energy (J).

b: Drone battery weight (kg).

WAER: The weighted mean emission rate of trucks = 1.2603 kg per mile = 0.787 kg per km.

PGFER: The level of CO_2 released by a power production facility per Wh used by a drone = 3.773 × 10–4 kg /Wh.

a: Energy consumption per kg of battery weight and load weight = 46.7 W per kg.

β: Energy required to keep the hexacopter frame in the air = 26.9 W.

Decision variables used in the formulation:

y_{ij}^{v}: Binary variable indicating that customer locations i and j are visited sequentially using truck v.

Z_i^v: Binary variable implying that truck v serves location i.

g_i^v: Cumulative load of trucks v at customer location i (kg).

gd_i^{vd}: Remaining load on drone d at customer location i (kg).

a_i^v : Cumulative time required of truck v at customer location i (h).

a_i^{vd} : Cumulative time required of drone d at customer location i (h).

y_{ij}^{vd}: Binary variable implying that customer locations i and j are visited sequentially by drone d deployed from truck v.

$y1_i^{vd}$: Binary variable implying that drone d is launched by truck v at location i.

$y2_i^{vd}$: Binary variable implying that drone d rejoins truck v at location i.

$y3_i^{vd}$: Binary variable implying that the drone owned by truck v serves location i.

f^{vd} : The maximum value of the accumulated energy expenditure of drone d owned by truck v (J).

f_i^{vd}: The cumulative total energy expenditure of drone d owned by truck v when it arrives at customer location i (J).

$P(m_i)^{vd}$: The power expenditure of drone *d* owned by truck *v*, associated with the total weight *m* (battery and load weight) at customer location *i* (W).

m_i^{vd}: Battery and load weight at customer location *i* (kg).

T^v: Total travel time of truck *v* between the depot and its return (h).

T^{vd}: Total travel time of drone *d* owned by truck *v* (h).

This study seeks to reduce the total number of round-trip truck journeys from the depot and the carbon footprint of the route. Objective 1 (f_1) is to minimize the travel time of trucks, as described in:

$$\sum_{v\epsilon V} T^v \quad (1)$$

Objective 2 (f_2) is to minimize the carbon footprint of truck and drone routes, as described in (2) and (3), respectively. Carbon emissions are estimated using the methodology from [26], where the total distance covered by the truck is used to compute its carbon emissions. Equation (2) calculates the total amount of carbon emissions from the truck, and (3) provides the calculation for the drone's overall carbon emissions:

$$\sum_{i\epsilon N}\sum_{j\epsilon N}\sum_{v\epsilon V} WAER * d_{ij} * y_{ij}^v \quad (2)$$

$$\sum_{v\epsilon V}\sum_{d\epsilon D} PGFER * f^{vd} * 1/3600 \quad (3)$$

Instead of using the AER value (drone energy requirement in Wh per mile), the model will use an energy expenditure expression relying on the drone's load and the distance it travels. The energy expenditure model used complies with [22].

The battery weight and the load weight at the customer point *i* are calculated by:

$$m_i^{vd} = b + gd_i^{vd} \quad (4)$$

Equation (5) is applied to determine how much the power expenditure of the drone associated with the total weight *m* at customer location *i* is:

$$P(m_i)^{vd} = \alpha * m_i^{vd} + \beta \quad (5)$$

The mathematical formulation of the 2E VRP-D model is:

$$\text{Min } (f_1, f_2) \quad (6)$$

Subsequently, the constraints associated with both objective functions are formulated as:

$$T^v \geq a_i^v + T_{i0(r)} \quad \forall i \epsilon C;\ \forall v \epsilon V \quad (7)$$

$$T^{vd} \geq a_j^v - a_i^v + \left(y1_i^{vd} + y2_j^{vd} - 2\right)M \quad \forall i \epsilon C;\ \forall j \epsilon C;\ \forall v \epsilon V;\forall d \epsilon D \quad (8)$$

$$\sum_{v\epsilon V} Z_i^v + \sum_{v\epsilon V}\sum_{d\epsilon D} y3_i^{vd} = 1 \quad \forall i \epsilon C \quad (9)$$

$$\sum_{j\epsilon C_+}\sum_{v\epsilon V} y_{ij}^v + \sum_{j\epsilon C}\sum_{v\epsilon V}\sum_{d\epsilon D} y_{ij}^{vd} \geq 1 \quad \forall i \epsilon C \quad (10)$$

$$\sum_{i\epsilon C_0}\sum_{v\epsilon V} y_{ij}^v + \sum_{i\epsilon C}\sum_{v\epsilon V}\sum_{d\epsilon D} y_{ij}^{vd} \geq 1 \quad \forall j \epsilon C \quad (11)$$

$$\sum_{i\epsilon C_0} y_{ik}^v - \sum_{j\epsilon C+} y_{kj}^v = 0 \quad \forall k \epsilon C;\ \forall v \epsilon V \quad (12)$$

$$\sum_{i\epsilon C} y_{0(s)i}^v \leq 1 \quad \forall v \epsilon V \quad (13)$$

$$\sum_{i\epsilon C} Z_i^v\, G_i + \sum_{i\epsilon C}\sum_{d\epsilon D} y3_i^{vd}\, G_i \leq Q^v \quad \forall i \epsilon C \quad (14)$$

$$a_j^v \geq a_i^v + T_{ij} + \left(y_{ij}^v - 1\right)M \quad \forall i \epsilon N;\ \forall j \epsilon N;\ \forall v \epsilon V;\forall d \epsilon D \quad (15)$$

$$y_{ij}^v + \sum_{d\epsilon D} y_{ij}^{vd} \leq 1 \quad \forall i \epsilon N;\ \forall j \epsilon N;\ \forall v \epsilon V \quad (16)$$

$$y_{ij}^{vd} + y_{ji}^{vd} \leq 1 \quad \forall i \epsilon N;\ \forall j \epsilon N;\ \forall v \epsilon V;\forall d \epsilon D \quad (17)$$

$$\sum_{i\epsilon N} y_{ik}^{vd} + y1_k^{vd} - \sum_{j\epsilon N} y_{kj}^{vd} - y2_k^{vd} = 0 \quad \forall k \epsilon N;\ \forall v \epsilon V;\forall d \epsilon D \quad (18)$$

$$\sum_{j\epsilon C}\sum_{v\epsilon V}\sum_{d\epsilon D} y_{ij}^{vd} \leq 1 \quad \forall i \epsilon C \quad (19)$$

$$\sum_{i\epsilon C}\sum_{v\epsilon V}\sum_{d\epsilon D} y_{ij}^{vd} \leq 1 \quad \forall j \epsilon C \quad (20)$$

$$\sum_{j\epsilon C} y_{0(s)j}^{vd} = 0 \quad \forall v \epsilon V;\forall d \epsilon D \quad (21)$$

$$\sum_{i\epsilon C} y3_i^{vd}\, G_i \leq Q^d \quad \forall v \epsilon V;\forall d \epsilon D \quad (22)$$

$$y1_i^{vd} \geq \sum_{j\epsilon N} y_{ij}^{vd} - \left(1 - \sum_{k\epsilon N} y_{ki}^v\right) \quad \forall i \epsilon N;\ \forall v \epsilon V;\forall d \epsilon D \quad (23)$$

$$y1_i^{vd} \leq \sum_{k\epsilon N} y_{ki}^v \quad \forall i \epsilon N;\ \forall v \epsilon V;\forall d \epsilon D \quad (24)$$

$$y1_i^{vd} \leq \sum_{j\epsilon N} y_{ij}^{vd} \quad \forall i \epsilon N;\ \forall v \epsilon V;\forall d \epsilon D \quad (25)$$

$$y2_i^{vd} \geq \sum_{j\epsilon N} y_{ji}^{vd} - \left(1 - \sum_{k\epsilon N} y_{ik}^v\right) \quad \forall i \epsilon N;\ \forall v \epsilon V;\forall d \epsilon D \quad (26)$$

$$y2_i^{vd} \leq \sum_{k\epsilon N} y_{ik}^v \quad \forall i \epsilon N;\ \forall v \epsilon V;\forall d \epsilon D \quad (27)$$

$$y2_i^{vd} \leq \sum_{j\epsilon N} y_{ji}^{vd} \quad \forall i \epsilon N;\ \forall v \epsilon V;\forall d \epsilon D \quad (28)$$

$$\sum_{i\epsilon N} y1_i^{vd} - \sum_{j\epsilon N} y2_j^{vd} = 0 \quad \forall v \epsilon V;\forall d \epsilon D \quad (29)$$

$$y3_i^{vd} \geq \sum_{j\epsilon N} y_{ji}^{vd} + \sum_{k\epsilon N} y_{ik}^{vd} - 1 \quad \forall i \epsilon N;\ \forall v \epsilon V;\forall d \epsilon D \quad (30)$$

$$y3_i^{vd} \leq \sum_{k\epsilon N} y_{ji}^{vd} \quad \forall i \epsilon N;\ \forall v \epsilon V;\forall d \epsilon D \quad (31)$$

$$y3_i^{vd} \leq \sum_{j\epsilon N} y_{ik}^{vd} \quad \forall i \epsilon N;\ \forall v \epsilon V;\forall d \epsilon D \quad (32)$$

$$a_j^{vd} \geq a_i^{vd} + T_{ij}^d + \left(y_{ij}^{vd} - 1\right)M \quad \forall i \epsilon N;\ \forall j \epsilon N;\ \forall v \epsilon V;\forall d \epsilon D \quad (33)$$

$$a_j^{vd} \geq a_j^v + \left(y1_j^{vd} - 1\right)M \quad \forall j \epsilon N;\ \forall v \epsilon V;\forall d \epsilon D \quad (34)$$

$$a_j^v \geq a_j^{vd} + \left(y2_j^{vd} - 1\right)M \quad \forall j \epsilon N;\ \forall v \epsilon V;\forall d \epsilon D \quad (35)$$

$$a_j^v + \left(1 - y2_j^{vd}\right)M \geq a_i^v + \left(y1_i^{vd} - 1\right)M \quad \forall i \epsilon N;\ \forall j \epsilon N;\ \forall v \epsilon V;\forall d \epsilon D \quad (36)$$

$$\sum_{v\epsilon V}\sum_{d\epsilon D} y1_i^{vd} + y2_i^{vd} \leq 1 \quad \forall i \epsilon N \quad (37)$$

$$gd_i^{vd} \geq \sum_{j\epsilon N} y3_j^{vd}\, G_j + \left(y1_i^{vd} - 1\right)M \quad \forall i \epsilon N;\ \forall j \epsilon N;\ \forall v \epsilon V;\forall d \epsilon D \quad (38)$$

$$gd_j^{vd} \geq gd_i^{vd} - G_j + \left(y_{ij}^{vd} - 1\right)M \quad \forall i \epsilon N;\ \forall j \epsilon N;\ \forall v \epsilon V;\forall d \epsilon D \quad (39)$$

$$f_i^{vd} \geq 0 + \left(y1_i^{vd} - 1\right)M$$

$$\forall i \in N; \forall v \in V; \forall d \in D \quad (40)$$

$$f_j^{vd} \geq f_i^{vd} + P(m_i)^{vd}\, T_{ij}^{d}\ 3600 + \left(y_{ij}^{vd} - 1\right) M \quad \forall i \in N;\ \forall j \in N;\ \forall v \in V; \forall d \in D \quad (41)$$

$$f^{vd} \geq f_i^{vd} \quad \forall i \in N; \forall v \in V; \forall d \in D \quad (42)$$

$$\geq f^{vd} \quad \forall v \in V; \forall d \in D \quad (43)$$

The model's objective function (6) is to reduce the trucks' round-trip travel time from the depot and to lower the overall carbon emissions. The complete travel duration for each truck and each drone can be seen in (7) and (8), respectively. Equation (9) stipulates that every customer location is assigned to the truck or drone for service. Equation (10) guarantees that both the truck and drone delivery routes must leave every customer location at least once, while (11) ensures that they must enter each customer point at least once. Equation (12) ensures truck route flow conservation. Equation (13) limits each truck to a single departure from the depot, and (14) restricts the combined truck and drone load to the truck's capacity limit. Equation (15) calculates the accumulated visit time for each truck at the customer location, (16) prevents the overlap between the truck and drone routes, (17) prevents the subtours in the drone's route, and (18) ensures drone route flow conservation. Equation (19) ensures that the drone leaves each customer location at most once, while (20) ensures that the drone enters each customer location at most once. Equation (21) enforces that the drone must not start its route from the depot, and (22) restricts the drone's payload to its capacity limit.

Equation (23) defines the variable $y1_i^{vd}$, representing the drone's departure location from the truck. Equation (24) stipulates that if a drone is dispatched from location *i*, the location must also be included in a truck route, while (25) requires that a drone route must also pass through the same location. Equation (26) defines the variable $y2_i^{vd}$, representing the location at which the drone reunites with the truck. Equation (27) guarantees that whenever the drone returns to the truck at location *i*, the location is included in a truck route, and (28) ensures that a drone route must also pass through it. Equation (29) enforces that the drone rejoins its originating truck, and (30) defines a variable $y3_i^{vd}$, indicating whether the drone serves location *i*. Equation (31) ensures that if a drone serves location i, an inbound route to i exists, while (32) ensures an outbound route from i. Equation (33) calculates the accumulated time of drone visits at each customer location. Equation (34) guarantees that the drone departs from location *j* only after the truck has arrived there, while (35) ensures that during rejoining, the moment when the truck reaches location *j* must be later than the drone's arrival time. Equation (36) enforces that the drone's departure time precedes its rejoining time, and (37) restricts each customer location so that it is either a drone departure point or a rejoining point but not both. Equation (38) calculates the total payload carried by the drone at its departure location, while (39) calculates the remaining payload after servicing a customer at location *j*. Equation (40) states that the accumulated energy consumed by the drone at point *i* is zero if *i* is a departure location. Equation (41) calculates the accumulated energy consumption of the drone at each visited location, and (42) determines the drone's total energy consumption after completing a delivery route. Equation (43) ensures that the energy expenditure for each drone assigned to a truck does not surpass its maximum available energy.

III. PROPOSED METHOD

Due to the absence of a single solution that can optimize all conflicting objectives at once, NSGA-II seeks to generate a Pareto-optimal set where the improvement of one objective results in the deterioration of another [19]. Specifically, NSGA-II employs a fast non-dominated sorting procedure to classify solutions into different Pareto fronts based on dominance relations. The solutions in the first front represent non-dominated solutions, while subsequent fronts contain dominated solutions. Additionally, a crowding distance mechanism is used to preserve diversity among solutions within the same front. During the selection process, individuals are chosen based on their rank (front level) and crowding distance, ensuring both convergence toward the Pareto-optimal front and diversity of solutions.

This research employs two different NSGA-II-based approaches. The first proposed approach uses a Giant Chromosome (GC), as proposed in [19], which contains all customer nodes to be served. Randomization through crossover and mutation is performed, followed by the allocation of customers to trucks using a truck route splitting algorithm. For each truck route, a corresponding drone route is then created using the newly developed heuristics in the drone route construction algorithm.

The second approach assigns customers to trucks using the K-means method. Randomization through crossover and mutation is then applied to the chromosomes formed within each cluster. The routing solution, comprising both the truck and drone paths, is obtained using a drone route construction algorithm. The framework of NSGA-II is depicted in Figures 2 and 3.

A. Encoding and Decoding

The GC contains all customer nodes, where crossover and mutation processes are performed. As shown in Figure 4, drone routes are obtained using the truck route splitting algorithm. Subsequently, drone routes and modified truck routes are constructed using the drone route construction algorithm. In this example, the GC is {2, 4, 14, 1, 6, 11, 8, 3, 15, 10, 5, 7, 12, 9, 13}, and the resulting truck routes 1 and 2 are {2, 14, 1, 3, 10, 5, 12, 13} and {4, 6, 11, 8, 15, 7, 9}, respectively. Furthermore, by applying the drone route construction algorithm to truck route 1, drone route 1 is obtained as {14, 1, 3, 10}, and drone route 2 as {5, 12, 13}. For truck route 2, only one drone route is obtained, namely {6, 8, 15, 7}. Since customers 1, 3, 12, 8, and 15 are served by drones, the modified truck routes become {2, 14, 10, 5, 13} for truck 1 and {4, 6, 11, 7, 9} for truck 2.

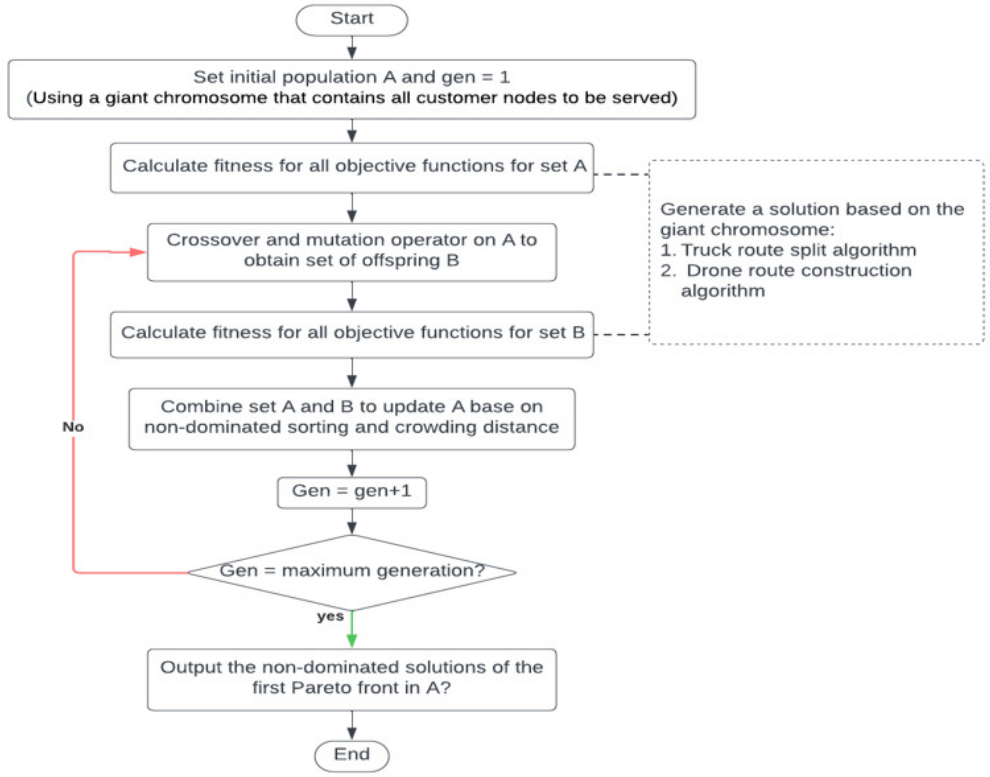

Fig. 2. Framework of the NSGA-II approach based on the GC representation.

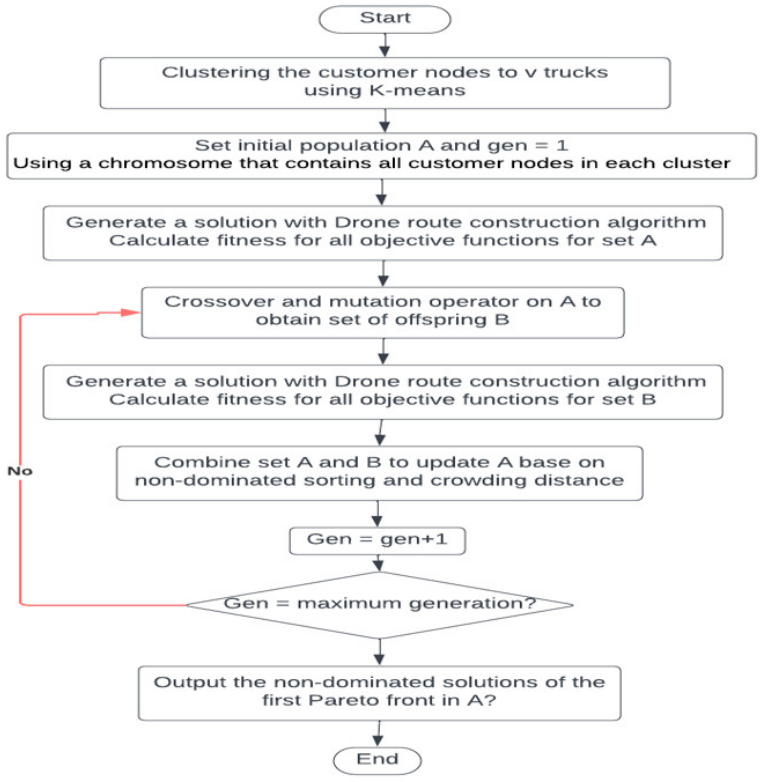

Fig. 3. The NSGA-II framework incorporating K-means clustering for preprocessing.

In the K-means-based approach, customer nodes are initially partitioned into clusters using the K-means algorithm. Crossover and mutation operations are then applied within each cluster. As displayed in Figure 5, two clusters are formed: {2, 14, 1, 3, 10, 5, 12, 13} and {4, 6, 11, 8, 15, 7, 9}. The drone and truck routes are subsequently generated using the drone route construction algorithm. The delivery routes for both trucks and drones are illustrated in Figure 6.

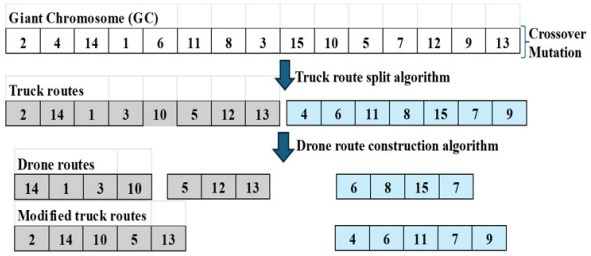

Fig. 4. Illustration of encoding and decoding for the GC approach.

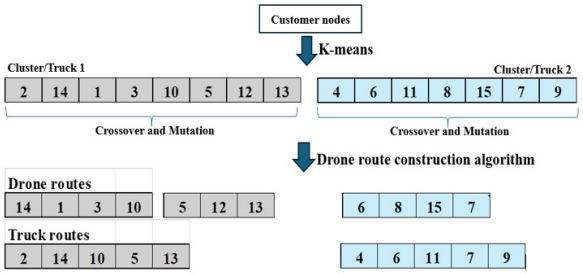

Fig. 5. Illustration of encoding and decoding for the K-means approach.

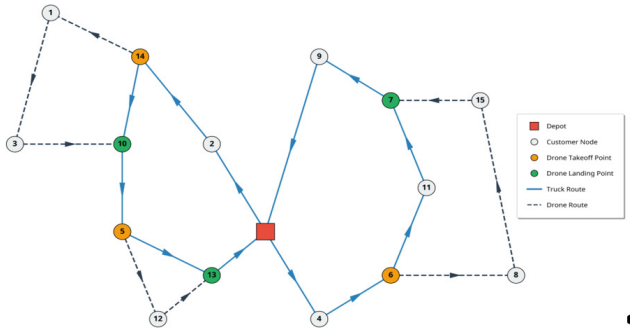

Fig. 6. Illustration of truck and drone delivery routes generated in the example.

B. Truck Route Split Algorithm

The service strategy required that all customer orders be fulfilled within a single day. The required truck fleet is computed from the total demand in relation to the truck carrying capacity. Customers are allocated to each truck based on its load capacity, in a way that reduces travel distance.

Step 1: All customer nodes on the GC will be distributed among the trucks to be used. For example, if three trucks are required, the first three customer nodes (genes) on the left side of the giant route will be assigned to the three trucks in sequence. Next, evaluate the load of each truck along with the distance to its assigned customer from the depot.

Step 2: The customer location in the fourth position on the giant route will be assigned to the truck with the smallest total mileage. If two or more trucks have the same total mileage, the customer will be assigned to one of them at random. Update the cumulative load and the traveled distance for each truck while maintaining the load within capacity.

Step 3: Continue iterating step two until every customer on the giant route is assigned to a truck.

C. K-Means Algorithm

At this stage, customers are assigned to different clusters using the K-means clustering method, with each cluster being served by the same truck. K-means remains one of the most popular and widely used clustering algorithms. Customers are grouped into multiple clusters based on homogeneous truck load capacity and their location coordinates. In this work, k-means clustering is used as an initial heuristic rather than a standalone contribution, aiming to improve the performance of the optimization process.

D. Drone Route Construction Algorithm

This algorithm is designed to build feasible drone routes that handle the maximum possible delivery tasks. This approach reduces the load and distance traveled by trucks, thereby decreasing the truck's travel time and total carbon emissions.

Step 1: For each truck, two sub-chromosomes will be created: the truck customer sub-chromosome (T sub-chromosome) and the drone customer sub-chromosome (D sub-chromosome). Customers whose demand exceeds the drone's load capacity will be served by trucks and are called truck customers. The truck customers' sub-chromosome will be sorted using the nearest-neighbor method, where the leftmost customer is randomly selected as the starting point for the nearest-neighbor process. This approach minimizes the distance traveled by the truck, thereby reducing the truck's travel time and carbon emissions produced by the truck.

Step 2: Take the first customer location on the T sub-chromosome as the drone's take-off point for the first drone route. Find the drone customer on the D sub-chromosome that is closest to the predetermined take-off point and form a temporary drone route consisting of the take-off point followed by the selected drone customer. This strategy is intended to shorten the drone's route. Ensure that the drone's load and the energy required do not exceed its carrying capacity and battery energy (E), respectively. Select the next drone customer and repeat this process until one of the requirements is not met. Discard the last drone customer that causes one or both of the requirements to be violated. The final drone customer's location will be the landing point, thus forming the complete drone route. Finally, calculate the drone's landing time.

Step 3: From the drone's take-off point in step two, the truck's route is built by adding customers one by one from the T sub-chromosome. The intention is to have the truck reach the landing point at a time that closely matches the drone's arrival.

Step 4: To generate a new drone route, sub-chromosomes T and D must contain a minimum of three customers,

representing the take-off point, the drone's service customers, and the landing point. If there are no customers in sub-chromosome T, the take-off point is determined by selecting the customer in sub-chromosome D that is closest to the landing location of the most recently created drone route. The process of creating the drone route will follow the same procedure as in step two. If leftover customers cannot be arranged into a drone route, they will be assigned to the truck and inserted at the end of the sequence. The remaining customer locations from sub-chromosome T will be placed first, followed by the remaining customer locations from sub-chromosome D.

E. Crossover and Mutation

In NSGA-II, the crossover technique used is Partially Matching Crossover (PMX), while the mutation techniques employed are swap, insertion, and reversal. This mutation process is repeated three times, each using one of three techniques. The crossover and mutation techniques are adopted from [19].

F. Performance Evaluation

Several metrics can be employed to evaluate the quality of Pareto fronts generated by optimization algorithms. In this study, the performance is assessed using Hypervolume (HV), Spacing, and Spread. The HV serves as a unary metric for comparing Pareto fronts produced by multi-objective optimization algorithms [27]. A larger HV value reflects better performance, as it represents a greater volume between the reference point and the Pareto front. All solution sets are normalized to fall within the interval [0, 1], and the resulting HV values also lie within this range. Since all objective functions are normalized within the range [0,1] and formulated as minimization problems, the reference point for HV calculation is set to (1, 1), which represents the worst possible values of the objectives. This ensures that all non-dominated solutions contribute to the HV metric.

Spacing quantifies the variation in distances among solutions within a set [20]. This metric should be minimized, as smaller spacing values indicate better performance. Specifically, a lower spacing value reflects a more uniform distribution of solutions across the objective space. Spacing is mathematically defined as:

$$S = \sqrt{\frac{1}{N-1}\sum_{i=1}^{N}\left(d_i - \bar{d}\right)^2} \quad (44)$$

where d_i represents the minimum distance between solution i and any other solution in the objective space, and $\bar{d}$ denotes the average of all d_i values. A spacing value of zero signifies a perfectly uniform distribution among solutions.

The spread metric (Δ) assesses both the extent and the uniformity of distribution along the Pareto front by accounting for the distances between adjacent solutions as well as the dispersion of extreme points [28]. It is defined as:

$$\Delta = \frac{d_f + d_l + \sum_{i=1}^{N-1}|d_i - \bar{d}|}{d_f + d_l + (N-1)\bar{d}} \quad (45)$$

where d_f and d_l represent the distances to the extreme solutions, d_i denotes the distance between consecutive solutions, and $\bar{d}$ is their mean. A smaller value of Δ indicates a better level of diversity and a more uniform distribution of solutions, with $\Delta = 0$ corresponding to an ideal Pareto front.

IV. RESULTS AND DISCUSSION

The performance of NSGA-II is evaluated using a new benchmark example designed to simulate real-world delivery scenarios [19]. The NSGA-II algorithm is implemented in MATLAB version R2023b and runs on a laptop with Windows 10, a 64-bit Intel i3 (4th generation) processor, and 12 GB of RAM. To simulate different area sizes, all depots and customers are located within a square-shaped region, where the vertical gap from the boundary to the center of the area takes values of 20, 30, or 40 km. The model is tested with 120 and 160 customers. The average speed of the trucks is 30 km/h, while the average speed of drones is 65 km/h [29]. The maximum allowable load for the truck is 1,000 kg [19]. The maximum load capacity of the drone is set to 20 kg [10]. Drone battery weight is 5 kg [9]. The battery capacity of the drone is set to 1,524,960 J [10]. In this study, NSGA-II uses specific parameter settings, including 50 iterations, a population size of 40, and genetic operators set at 0.9 for crossover and 0.1 for mutation. Since these examples involve different combinations (number of customers and vertical area size), they will henceforth be labeled (120-20), which corresponds to 120 customers and an area size of 20 km.

Each instance was subjected to six runs under the NSGA-II algorithm to obtain consistent performance results. Table I presents the average and standard deviations of truck travel time and carbon emissions for all instances. Table II depicts the differences in truck travel time and carbon emissions between the two approaches for all instances. Moreover, HV, Spacing, and Spread are applied as quality indicators to evaluate the solution set of the proposed multi-objective algorithm. The average values of HV, Spacing, and Spread for both approaches across all test instances are reported in Table III.

For each run, the best objective function value is obtained by selecting the most favorable non-dominated solution based on the crowding distance. The values outlined in Table I correspond to the averages over all runs. The GC approach demonstrates a longer computation time, primarily due to its broader exploration of the solution space. In contrast, the K-means approach achieves faster computation times by employing a preprocessing step that partitions customers into clusters, although this may limit the search space. Table II shows that the K-means approach achieves better results for both objective functions. Overall, the K-means approach performs 20.356% better in terms of truck travel time and 16.577% better in terms of carbon emissions.

Although the K-means approach achieves better results for both objective functions across all instances, Table III shows that its HV value is superior only for the 120-20 instance. The average objective values are better; however, the HV may be lower due to the limited diversity and coverage of the Pareto front. Even though the K-means approach achieves better

average objective values, the GC approach produces a larger HV, indicating superior diversity and coverage of the Pareto front. This suggests that the GC approach is more effective in approximating the true Pareto front, while the K-means approach is more focused on obtaining locally optimal solutions. Figure 7 presents a Pareto front example for the 160-20 instance generated by both approaches. The GC approach achieves a higher HV (0.919) than the K-means approach (0.897), indicating a higher-quality Pareto front despite lower average objective values.

The results indicate that the use of K-means as a preprocessing step reduces computational time and improves the objective function value. However, it leads to a smaller HV compared to the approach without clustering (i.e., using the GC representation). This suggests that while preprocessing enhances efficiency and solution quality in a single-objective sense, it may limit solution diversity in the multi-objective space.

A similar observation can be noted in the spacing metric, where GC demonstrates better performance (0.066) than K-means (0.117). This indicates that the solutions generated by GC are more evenly distributed along the Pareto front, while K-means tends to produce clustered solutions with uneven gaps. This behavior is expected, as the clustering preprocessing step restricts the search space and biases the algorithm toward certain regions. On the other hand, the K-means approach shows better performance in terms of spread (0.622) compared to GC (0.686), indicating a more controlled and stable distribution of solutions. This suggests that although K-means sacrifices diversity, it maintains consistency and avoids extreme variations among solutions.

TABLE I. AVERAGE AND STANDARD DEVIATION OF TRUCK TRAVEL TIME AND TOTAL CARBON EMISSIONS

Instance	Number of trucks	GC					K-means				
		Computation time (s)	Truck travel time (h)		Total carbon emission (kg)		Computation time (s)	Truck travel time (h)		Total carbon emission (kg)	
			Average	St. dev.	Average	St. dev.		Average	St. dev.	Average	St. dev.
120-20	3	472.371	19.618	0.245	369.527	3.599	450.184	15.147	0.186	304.073	1.183
120-30	3	571.240	31.434	0.332	623.367	4.126	466.588	24.476	0.913	531.304	16.215
120-40	3	583.244	36.100	0.501	744.085	18.824	476.633	32.689	2.186	620.543	4.969
160-20	3	850.546	30.400	1.115	566.357	9.544	732.395	23.344	1.228	445.157	7.727
160-30	3	1,061.693	40.191	0.813	701.878	19.406	864.674	29.060	0.460	592.264	5.830
160-40	3	1,323.503	63.138	1.305	1,151.404	19.165	969.908	52.497	2.902	997.572	22.642

TABLE II. DIFFERENCE IN TRUCK TRAVEL TIME AND CARBON EMISSIONS BETWEEN THE GC AND K-MEANS APPROACHES

Instance	Truck travel time difference	Carbon emission difference
120-20	22.791 %	17.713 %
120-30	22.135 %	14.769 %
120-40	9.449 %	16.603 %
160-20	23.211 %	21.400 %
160-30	27.695 %	15.617 %
160-40	16.854 %	13.360 %
Average	20.356 %	16.577 %
Standard deviation	6.361 %	2.796 %

TABLE III. COMPARISON OF HV, SPACING, AND SPREAD VALUES BETWEEN GC AND K-MEANS APPROACHES

Instance	GC			K-means		
	HV	Spacing	Spread	HV	Spacing	Spread
120-20	0.835	0.043	0.548	0.929	0.045	0.615
120-30	0.868	0.046	0.611	0.850	0.181	0.545
120-40	0.938	0.011	0.673	0.904	0.187	0.715
160-20	0.955	0.107	0.804	0.930	0.012	0.640
160-30	0.958	0.124	0.817	0.867	0.117	0.630
160-40	0.957	0.064	0.663	0.904	0.160	0.584
Average	0.919	0.066	0.686	0.897	0.117	0.622
St.dev	0.053	0.042	0.106	0.033	0.074	0.057

These findings highlight a significant trade-off in multi-objective optimization. The K-means approach emphasizes exploitation, focusing on improving objective function values and producing efficient solutions. In contrast, the GC approach emphasizes exploration, enabling a broader search of the solution space and generating a more diverse set of Pareto-optimal solutions. This suggests that future research could explore hybrid strategies that balance exploration and exploitation, potentially combining clustering-based initialization with diversity-preserving mechanisms to achieve both high-quality and well-distributed Pareto solutions.

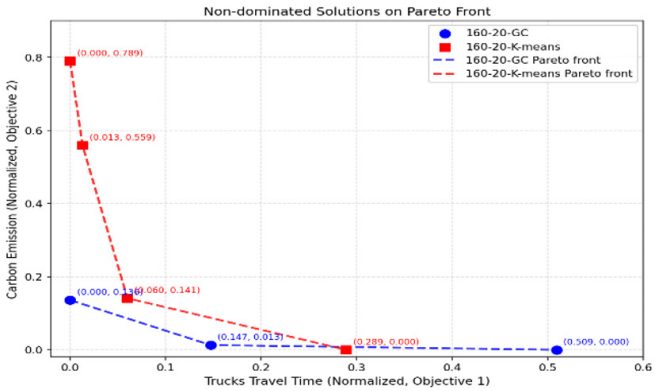

Fig. 7. Plot of the Pareto front obtained, for instance, 160-20.

V. CONCLUSION

To assist logistics providers in evaluating trade-offs between cost and ecological concerns, this study develops a multi-objective Two-Echelon Vehicle Routing Problem with Drones (2E VRP-D) model that integrates drone energy consumption considerations. This study is designed to minimize the total time required for truck travel while also reducing total carbon emissions, which is expected to identify fast delivery routes and help minimize the environmental

impact of delivery. Energy consumption in this 2E VRP-D model is represented as a function of load and distance. This study integrates the Non-Dominated Sorting Genetic Algorithm (NSGA-II) to handle multi-objective optimization.

The Hypervolume (HV) values obtained by both approaches are considered good, as all values exceed 0.83, indicating a strong ability to approximate the Pareto front. For spacing, the Giant Chromosome (GC) approach (0.066) falls within the good range (< 0.1), reflecting a relatively uniform distribution of solutions, while the K-means approach (0.117) is still acceptable but indicates less uniformity. In terms of spread, both approaches produce values within the acceptable range (0.5–0.7), with K-means (0.622) showing better diversity stability compared to GC (0.686), although the latter is close to the upper limit.

The performance can be significantly improved by incorporating hybrid heuristic methods, including local and tabu search, to enhance convergence. Additionally, several real-world factors can be considered, such as the existence of no-fly zones and uncertain customer demand.

DECLARATION OF COMPETING INTERESTS

The authors state no conflict of interest.

ACKNOWLEDGMENT

The authors gratefully acknowledge the financial support provided by Universitas Kristen Maranatha and research support from Institut Teknologi Sepuluh Nopember.

DATA AVAILABILITY

The data supporting the findings of this study are available from the corresponding author upon reasonable request.

REFERENCES

[1] S. Lichau, R. Sadykov, J. François, and R. Dupas, "A branch-cut-and-price approach for the two-echelon vehicle routing problem with drones," *Computers & Operations Research*, vol. 173, Jan. 2025, Art. no. 106869, https://doi.org/10.1016/j.cor.2024.106869.

[2] P. Kitjacharoenchai, B.-C. Min, and S. Lee, "Two echelon vehicle routing problem with drones in last mile delivery," *International Journal of Production Economics*, vol. 225, July 2020, Art. no. 107598, https://doi.org/10.1016/j.ijpe.2019.107598.

[3] S. M. Ferrandez, T. Harbison, T. Weber, R. Sturges, and R. Rich, "Optimization of a truck-drone in tandem delivery network using k-means and genetic algorithm," *Journal of Industrial Engineering and Management*, vol. 9, no. 2, 2016, Art. no. 374, http://dx.doi.org/10.3926/jiem.1929.

[4] G. Macrina, L. Di Puglia Pugliese, F. Guerriero, and G. Laporte, "Drone-aided routing: A literature review," *Transportation Research Part C: Emerging Technologies*, vol. 120, Nov. 2020, Art. no. 102762, https://doi.org/10.1016/j.trc.2020.102762.

[5] X. Han, Q. Spring Zhou, B. Bobby Du, and J. Shen, "Two- Echelon Vehicle Routing Problem with Trucks and Drones," in *2024 Twelfth International Conference on Advanced Cloud and Big Data* (*CBD*), Brisbane, Australia, Nov. 28 – Dec. 02, 2024, pp. 290–295, https://doi.org/10.1109/CBD65573.2024.00059.

[6] Z. Wang and J.-B. Sheu, "Vehicle routing problem with drones," *Transportation Research Part B: Methodological*, vol. 122, pp. 350–364, Apr. 2019, https://doi.org/10.1016/j.trb.2019.03.005.

[7] H. Li, H. Wang, J. Chen, and M. Bai, "Two-echelon vehicle routing problem with time windows and mobile satellites," *Transportation Research Part B: Methodological*, vol. 138, pp. 179–201, Aug. 2020, https://doi.org/10.1016/j.trb.2020.05.010.

[8] Y. Lu, C. Yang, and J. Yang, "A multi-objective humanitarian pickup and delivery vehicle routing problem with drones," *Annals of Operations Research*, vol. 319, no. 1, pp. 291–353, 2022, https://doi.org/10.1007/s10479-022-04816-y.

[9] Z. Luo, R. Gu, M. Poon, Z. Liu, and A. Lim, "A last-mile drone-assisted one-to-one pickup and delivery problem with multi-visit drone trips," *Computers & Operations Research*, vol. 148, Dec. 2022, Art. no. 106015, https://doi.org/10.1016/j.cor.2022.106015.

[10] Y. Xia, W. Zeng, C. Zhang, and H. Yang, "A branch-and-price-and-cut algorithm for the vehicle routing problem with load-dependent drones," *Transportation Research Part B: Methodological*, vol. 171, pp. 80–110, May 2023, https://doi.org/10.1016/j.trb.2023.03.003.

[11] Y.-Q. Liu, J. Han, Y. Zhang, Y. Li, and T. Jiang, "Multivisit Drone-Vehicle Routing Problem with Simultaneous Pickup and Delivery considering No-Fly Zones," *Discrete Dynamics in Nature and Society*, vol. 2023, no. 1, 2023, Art. no. 1183764, https://doi.org/10.1155/2023/1183764.

[12] Q. Xiao and J. Gao, "The Multi-Visit Vehicle Routing Problem with Drones under Carbon Trading Mechanism," *Sustainability*, vol. 16, no. 14, 2024, Art. no. 6145, https://doi.org/10.3390/su16146145.

[13] Y. Liu, Z. Liu, J. Shi, G. Wu, and W. Pedrycz, "Two-Echelon Routing Problem for Parcel Delivery by Cooperated Truck and Drone," *IEEE Transactions on Systems, Man, and Cybernetics: Systems*, vol. 51, no. 12, pp. 7450–7465, Dec. 2021, https://doi.org/10.1109/TSMC.2020.2968839.

[14] S. Bansal, R. Goel, and R. Maini, "Ground vehicle and UAV collaborative routing and scheduling for humanitarian logistics using random walk based ant colony optimization," *Scientia Iranica. Transaction D, Computer Science & Engineering, Electrical*, vol. 29, no. 2, pp. 632–644, 2022, https://doi.org/10.24200/sci.2021.58309.5664.

[15] F. Zeng, Z. Chen, J.-P. Clarke, and D. Goldsman, "Nested vehicle routing problem: Optimizing drone-truck surveillance operations," *Transportation Research Part C: Emerging Technologies*, vol. 139, June 2022, Art. no. 103645, https://doi.org/10.1016/j.trc.2022.103645.

[16] J. Zhou, Q. Yu, Z. Xue, and L. Yang, "Research on the Route Planning Problem of Drone and Truck Collaborative Delivery in Restricted Areas," *IEEE Access*, vol. 13, pp. 33062–33073, 2025, https://doi.org/10.1109/ACCESS.2025.3540880.

[17] M. Yang, B. Xue, R. Zhang, and F. Dong, "A Hybrid Strategy-Assisted Cooperative Vehicles–Drone Multi-Objective Routing Optimization Method for Last-Mile Delivery," *Drones*, vol. 10, no. 1, Jan. 2026, Art. no. 7, https://doi.org/10.3390/drones10010007.

[18] F. Wei, X. Zhang, J. Chu, F. Yang, and Z. Yuan, "Energy and environmental efficiency of China's transportation sectors considering CO_2 emission uncertainty," *Transportation Research Part D: Transport and Environment*, vol. 97, Aug. 2021, Art. no. 102955, https://doi.org/10.1016/j.trd.2021.102955.

[19] S. Zhang, S. Liu, W. Xu, and W. Wang, "A novel multi-objective optimization model for the vehicle routing problem with drone delivery and dynamic flight endurance," *Computers & Industrial Engineering*, vol. 173, Nov. 2022, Art. no. 108679, https://doi.org/10.1016/j.cie.2022.108679.

[20] R. J. Kuo, E. Edbert, F. E. Zulvia, and S.-H. Lu, "Applying NSGA-II to vehicle routing problem with drones considering makespan and carbon emission," *Expert Systems with Applications*, vol. 221, July 2023, Art. no. 119777, https://doi.org/10.1016/j.eswa.2023.119777.

[21] A. A. Deshpande, S. Raut, and N. V. Vaidya, "Solving the Multi-objective Travelling Salesman Problem by an Amalgam of Fruit Fly Optimization and Ant Colony Optimization," *Engineering, Technology & Applied Science Research*, vol. 14, no. 4, pp. 15564–15569, Aug. 2024, https://doi.org/10.48084/etasr.7353.

[22] K. Dorling, J. Heinrichs, G. G. Messier, and S. Magierowski, "Vehicle Routing Problems for Drone Delivery," *IEEE Transactions on Systems, Man, and Cybernetics: Systems*, vol. 47, no. 1, pp. 70–85, Jan. 2017, https://doi.org/10.1109/TSMC.2016.2582745.

[23] E. Yakıcı, "A heuristic approach for solving a rich min-max vehicle routing problem with mixed fleet and mixed demand," *Computers & Industrial Engineering*, vol. 109, pp. 288–294, July 2017, https://doi.org/10.1016/j.cie.2017.05.001.

[24] S. Verma, M. Pant, and V. Snasel, "A Comprehensive Review on NSGA-II for Multi-Objective Combinatorial Optimization Problems," *IEEE Access*, vol. 9, pp. 57757–57791, 2021, https://doi.org/10.1109/ACCESS.2021.3070634.

[25] I. Khenissi, S. M. Alotaibi, M. T. Chughtai, and T. Guesmi, "An Improved Non-dominated Sorting Genetic Algorithm for the Optimal Economic Emission Dispatch Problem with Wind Power Sources," *Engineering, Technology & Applied Science Research*, vol. 14, no. 5, pp. 16970–16976, Oct. 2024, https://doi.org/10.48084/etasr.7171.

[26] W.-C. Chiang, Y. Li, J. Shang, and T. L. Urban, "Impact of drone delivery on sustainability and cost: Realizing the UAV potential through vehicle routing optimization," *Applied Energy*, vol. 242, pp. 1164–1175, May 2019, https://doi.org/10.1016/j.apenergy.2019.03.117.

[27] M. M. Drugan and D. Thierens, "Path-Guided Mutation for Stochastic Pareto Local Search Algorithms," in *Parallel Problem Solving from Nature, PPSN XI*, Krakow, Poland, Sept. 11–15, 2010, pp. 485–495, https://doi.org/10.1007/978-3-642-15844-5_49.

[28] K. Deb, A. Pratap, S. Agarwal, and T. Meyarivan, "A fast and elitist multiobjective genetic algorithm: NSGA-II," *IEEE Transactions on Evolutionary Computation*, vol. 6, no. 2, pp. 182–197, Apr. 2002, https://doi.org/10.1109/4235.996017.

[29] H. Li, H. Wang, J. Chen, and M. Bai, "Two-echelon vehicle routing problem with satellite bi-synchronization," *European Journal of Operational Research*, vol. 288, no. 3, pp. 775–793, Feb. 2021, https://doi.org/10.1016/j.ejor.2020.06.019.